



Selenium Exerts Protective Effects Against Fluoride-Induced Apoptosis and Oxidative Stress and Altered the Expression of Bcl-2/Caspase Family

Jiping Gao¹ · Xiaolin Tian^{2,3} · Xiaoru Yan¹ · Yu Wang¹ · Jianing Wei¹ · Xiaotang Wang¹ · Xiaoyan Yan² · Guohua Song^{1,4}

Received: 22 January 2020 / Accepted: 4 May 2020 / Published online: 1 July 2020
© Springer Science+Business Media, LLC, part of Springer Nature 2020

Abstract

Fluoride is widely distributed in nature, and at high concentrations, it targets the kidney and especially proximal tubule epithelial cells. Selenium is a typical trace element beneficial to humans, and the role of selenium in the prevention and treatment of fluoride-induced organ damage is an important research topic. The purpose of this study was to investigate the possible protective effects of selenium against fluoride-induced oxidative stress and apoptosis in rat renal tubular epithelial cells. We showed that the activity of antioxidant enzymes (superoxide dismutase and glutathione peroxidase) and total antioxidant capacity were significantly reduced in NaF-treated normal rat kidney cells (NRK-52E), whereas the levels of nitrogen monoxide (NO) and malondialdehyde (MDA) were significantly increased. Moreover, the number of apoptotic cells, mRNA expression of Bax, Bad, caspase-3, caspase-8, and caspase-9, and protein expression of Bax were elevated, while mitochondrial membrane potential and the protein expression of Bcl-2 were reduced. Compared with the NaF group, pretreatment with selenium enhanced the activity of antioxidant enzymes, mitochondrial membrane potential, and protein expression of Bcl-2, while the levels of NO and MDA, number of apoptotic cells, mRNA expression of Bax, Bad, caspase-3, caspase-8, and caspase-9, and protein expression of Bax were decreased. In conclusion, selenium exerted remarkable protective effect against NaF-induced oxidative stress and apoptosis and altered the expression of Bcl-2/caspase family.

Keywords Sodium fluoride · Selenium · NRK-52E cells · Oxidative stress · Apoptosis

Introduction

Fluoride is a naturally occurring compound that is widely used in various applications including pharmaceutical preparations, agricultural agents, pesticides, and surfactants [1]. According to the World Health Organization guidelines, the

recommended concentration of fluoride in drinking water is 1.0 mg/L with an upper limit of 1.5 mg/L [2]. Especially high fluoride concentrations in nature have been found in India, Mexico, Turkey, North Africa, and China (Yunnan and Guizhou provinces) [3]. Approximately 50–80% of the fluoride absorbed by the body is excreted through urine, primarily by glomerular filtration [4]. As a result, the kidney and especially proximal tubule epithelial cells are important targets for fluorine accumulation, drainage, and toxic effect [5]. Previous studies have demonstrated that fluoride induces oxidative stress by promoting aerobic metabolism and altering cellular free radicals while reducing the activity of antioxidant enzymes in the kidney [6–8]. Additionally, the ability of fluoride to initiate apoptosis in the kidney has been documented [9]. In an effort to prevent and treat fluoride nephrotoxicity, the effects of some antioxidant and anti-apoptosis compounds are currently being investigated.

Selenium is a typical trace element beneficial to human and animal health that participates in the protection against chronic kidney diseases [10]. The role of selenium in the prevention

✉ Guohua Song
ykdsgh@sxmu.edu.cn

¹ Laboratory Animal Center, Shanxi Key Laboratory of Experimental Animal Science and Human Disease Animal Model, Shanxi Medical University, Road Xinjian 56, Taiyuan 030001, China

² Shanxi Key Laboratory of Ecological Animal Science and Environmental Medicine, Shanxi Agricultural University, Taigu 030801, China

³ School of Public Health, Shanxi Medical University, Taiyuan 030001, Shanxi, China

⁴ Mental Health Hospital Affiliated to Shanxi Medical University, Street Nanshifang 55, Taiyuan City 030001, Shanxi Province, China

and treatment of certain diseases has drawn significant attention. Many reports have demonstrated the antagonistic effect of selenium against fluorosis, and the protective effect of sodium selenite has been confirmed in fluorosis-induced rats [11–14]. Therefore, the role of selenium in the prevention and treatment of fluorosis is an important research topic. Interestingly, recent research has shown that selenium is an essential component of glutathione peroxidase (GSH-px). Meanwhile, many studies have shown the antagonism of selenium against excessive oxidative stress and apoptosis [15, 16]. In this context, we investigated the protective effect of selenium against fluoride-induced oxidative stress and apoptosis.

We hypothesized that selenium exerts protective effects against sodium fluoride-induced toxicity in rat renal tubular epithelial cells. To verify this hypothesis, we established a cell model in which renal tubular epithelial cells were subjected to fluoride and selenium treatment. We evaluated the levels of superoxide dismutase (SOD), GSH-px, total antioxidant capacity (T-AOC), nitrogen monoxide (NO), and malondialdehyde (MDA), mitochondrial membrane potential ($\Delta\Psi_m$), degree of apoptosis, and expression of apoptosis-related proteins in the Bcl-2 and caspase family. The purpose of the present study was to investigate the possible protective effects of selenium against fluoride-induced oxidative stress and apoptosis in rat renal cells.

Materials and Methods

Chemicals and Reagents

NaF was obtained from the Tianjin Reagent Company (Tianjin, China). Na₂SeO₃ was purchased from the Tianjin Chemical Reagent Factory (Tianjin, China). Fetal calf serum was obtained from Hangzhou Sijiqing Biological Engineering Material Company (Hangzhou, China). Assay kits for SOD, MDA, NO, GSH-px, and T-AOC were purchased from Nanjing Jiancheng Biological Engineering Institute (Nanjing, China). The tetraethylbenzimidazolyl carbocyanine iodide (JC-1) assay kit was purchased from Beyotime Institute of Biotechnology (Cangzhou, China). The Annexin V-FITC apoptosis detection kit was purchased from Key GEN Bio TECH (Nanjing, China). Prime Script RT Master Mix and SYBR Primix Ex Taq were purchased from Taraka (Japan). All other chemicals and reagents were of analytical grade.

Cell Culture

The NRK-52E cells were purchased from the Type Culture Collection of the Chinese Academy of Sciences (Shanghai, China) and maintained in high-glucose Dulbecco's modified Eagle medium containing 10% fetal calf serum, 100 IU/mL

penicillin, and 100 g/mL streptomycin in an incubator containing 5% CO₂ at 37 °C. Medium was changed every 2 days, and cells in the logarithmic growth phase were used throughout the study. When the cells had grown to 70–80% confluence, they were exposed to NaF and Na₂SeO₃ at different concentrations (Table 1) and incubated for 48 h in medium containing 5% fetal calf serum.

Cell Proliferation Assay

We evaluated the proliferation of NRK-52E cells using the colorimetric 3-(4,5-dimethyl thiazol-2-yl)-2,5-diphenyltetrazolium bromide (MTT) assay. Cells were seeded in 96-well culture plates and incubated for 24 h. After the cells had adhered, they were cultured separately with different concentrations of NaF (0, 2.5, 5, 10, 20, and 40 mg/L) and Na₂SeO₃ (0, 8.5, 17.1, 34.2, 68.4, and 136.8 µg/L) for 0, 24, 48, 72, and 96 h, and six replicates were set up for each concentration. Subsequently, 10 µL of MTT solution was added, and the cells were further incubated for 4 h. Then, 100 µL of formazan lysate was added to each well and the absorbance was measured at 570 nm. Based on the absorbance value, the optimal concentration of the affected cells was screened.

Detection of Intracellular Oxidative Stress

We detected the oxidative stress index by determining the levels of SOD, MDA, NO, and GSH-pX and the T-AOC according to the instructions of the assay kits.

Detection of $\Delta\Psi_m$

Cells were cultured for 48 h according to Table 1. After treatment, the cells were trypsinized, collected by centrifugation, and suspended in complete Dulbecco's modified Eagle medium at $1-6 \times 10^5$ cells/mL. Then, 500 µL of JC-1 was added to the medium, and the cells were incubated for 20 min in 5%

Table 1 Experimental groups

Groups	NaF (mg/L)	Na ₂ SeO ₃ (µg/L)
Control	0	0
F	5	0
	20	0
Se	0	17.1
	0	34.2
F+Se	5	17.1
	5	34.2
	20	17.1
	20	34.2

CO₂ at 37 °C. The cells were then washed twice with JC-1 stain buffer solution (1×) after centrifugation at 600 rpm at 4 °C for 3–4 min. The cells were resuspended in 250 μL of JC-1 stain buffer solution (1×), and the ΔΨ_m was measured by flow cytometry (Becton Dickinson).

Apoptosis Assay

Cells were cultured for 48 h according to Table 1. After treatment, the cells were trypsinized, washed twice with phosphate-buffered saline (pH = 7.4), and resuspended in 500 μL of binding buffer at 1–5 × 10⁵ cells/mL. To each sample, 5 mL of Annexin V-fluorescein isothiocyanate (FITC) and 5 mL of propidium iodide (PI) solution were added, and the cells were incubated for 10 min in the dark. Quantitative analysis of cell apoptosis was performed using flow cytometry (Becton Dickinson). FITC and PI give off green and red fluorescence, respectively.

Quantitative Reverse Transcription Polymerase Chain Reaction (qRT-PCR)

Total RNA was extracted from rat renal tubular epithelial cells with TRIzol, and the purity of the RNA was determined using a microplate reader (Bio-Rad, USA). The mRNA expression of Bcl-2, Bad, Bax, caspase-3, caspase-8, and caspase-9 was detected with Prime Script RT Master Mix and SYBR Primix Ex Taq (Takara, Japan). β-actin was used as a reference. qRT-PCR (ABI, USA) was performed with a total volume of 20 μL, and the specific amounts of reagents are shown in Table 2. The specific primer sequences for Bcl-2, Bad, Bax, caspase-3, caspase-8, caspase-9, and β-actin were designed (Table 3). The reaction conditions were as follows: 95 °C for 30 s (preheating); 40 cycles of 95 °C for 5 s (denaturation); 60 °C for 31 s (annealing). The dissociation stage was analyzed.

Western Blot

After treatment, cells were harvested, washed with three times with phosphate-buffered saline, and lysed in 250 μL of ice-cold cell lysis buffer containing 2.5 μL phenylmethanesulfonyl

Table 3 Primer sequences for real-time PCR

Gene	Primer sequence
Bcl-2	F: 5'-GGAGGCTGGGATGCCTTTG-3' R: 5'-CTGAGCAGCGTCTTCAGAGACA-3'
Bax	F: 5'-CTCAAGGCCCTGTGCACTAAA-3' R: 5'-CCCGGAGGAAGTCCAGTGT-3'
bad	F: 5'-CGGGACAGGCAGCCAATA-3' R: 5'-CGACTCCGGGTCTCCATAGTC-3'
Caspase-3	F: 5'AGGCCGACTTCCTGTATGCTT-3' R: 5'TGACCCGTCCTTGAATTTC-3'
Caspase-9	F: 5'-GAGAGACATGCAGATATGGCATAACA-3' R: 5'-CAGAAGTTCACGTGTTGATGATG-3'
Caspase-8	F: 5'-CGAACGATCAAGCACAGAGAGA-3' R: 5'-CTGGCGAGTCCCACATGTC-3'
β-actin	F: 5'-AGCCATGTACGTAGCCATCC-3' R: 5'-ACCCTCATAGATGGGCACAG-3'

fluoride for 1–3 h. The protein content was estimated using a bicinchoninic acid assay kit. The protein samples containing loading buffer was separated by 10% sodium dodecyl sulfate-polyacrylamide gel electrophoresis and transferred to a nitrocellulose membrane. After blocking with 5% non-fat dry milk in Tris-buffered saline containing 0.1% Tween-20 and 5% bovine serum albumin (TBST) for 2 h at room temperature, the membrane was probed with primary antibodies against Bax, Bcl-2, and β-actin overnight at 4 °C. Then, the membranes were washed three times with TBST for 10 min and blotted with horseradish peroxidase-conjugated secondary antibodies. The immune bands were visualized with enhanced chemiluminescence, and imaging was performed using a gel imaging analyzer. Protein bands for Bax and Bcl-2 were analyzed using Quantity One 4.6.6 software.

Statistical Analysis

All data were expressed as the mean ± standard deviation. Statistical analysis was performed using SPSS software (version 19.0) with one-way analysis of variance followed by the least significant difference post hoc test to compare means between groups. *P* < 0.05 was considered statistically significant.

Table 2 Distribution system of real-time PCR

Reagent	Consumption (μl)	Concentration
SYBR® Premix Ex TaqII (Tli RNaseH Plus) (2×)	10	1 ×
PCR Forward Primer (10 μM)	0.8	0.4 μM*1
PCR Reverse Primer (10 μM)	0.8	0.4 μM*1
ROX Reference Dye (50×)	0.4	1 ×
RT solution (cDNA solution)	2	2
dH ₂ O	6	–

Results

Effect of NaF and Na₂SeO₃ on NRK-52E Cell Proliferation

The proliferation results of NRK-52E cells after exposure to NaF and Na₂SeO₃ for 0, 24, 48, 72, and 96 h was showed in Fig. 1). Compared with the control group, exposure to 5, 10, and 20 mg/L NaF for 24, 48, and 72 h significantly inhibited the proliferation of NRK-52E cells. Moreover, culture with NaF at 5 mg/L for 48 and 72 h suppressed cell proliferation compared with that of the control group. Interestingly, 96 h of exposure to all other concentrations of NaF except for 40 mg/L remarkably increased the proliferation of NRK-52E cells. Compared with the control group, exposure to 34.2 μg/L Na₂SeO₃ for 24 h remarkably increased the proliferation of NRK-52E cells, and exposure to 8.5 and 136.8 μg/L Na₂SeO₃ for 72 h significantly inhibited the proliferation of NRK-52E cells. Therefore, the exposure concentrations selected for subsequent studies were 5 and 20 mg/L for NaF and 17.1 and 34.2 μg/L for Na₂SeO₃, with an exposure time of 48 h.

Effect of NaF and/or Na₂SeO₃ on the Morphology of NRK-52E Cells

NRK-52E cells were treated with different concentrations of NaF and/or Na₂SeO₃ for 48 h. In the control and Na₂SeO₃ group without NaF, the NRK-52E cells grew vigorously, showing a large number of cells and natural morphology (Figs. 1 and 2 (A1–3)). With increasing NaF concentration (0, 5, and 20 mg/L), we observed clear abnormal changes in renal tubular epithelial cells. Cells treated with 5 mg/L NaF began to show enlarged cell volume and nuclei, wider intercellular space, and decreased cell adhesion (Fig. 2 (B1)). The number of cells decreased significantly, most of the cells showed cavitation, and the cell volume gradually increased after 48 h exposure to 20 mg/L NaF (Fig. 2 (C)). Interestingly, compared with the low NaF (5 mg/L) group, the cell morphology tended to be normal in the Na₂SeO₃ intervention group (Fig. 2 (B2–3)). This shift in NRK-52E cell morphology indicates that selenium repaired the morphology of renal tubular epithelial cells.

Effect of NaF and/or Na₂SeO₃ on the Level of SOD, GSH-Px, T-AOC, NO, and MDA

To investigate whether selenium alleviates damage caused by fluoride, we examined the levels of oxidative

stress indicators SOD, GSH-px, T-AOC, NO, and MDA in Fig. 3. The activity of antioxidant enzymes (SOD and GSH-px) and the T-AOC fell sharply in all groups exposed to high fluoride concentration (20 mg/L). Meanwhile, the content of NO, which reflects free radical levels, was significantly increased in all groups exposed to high fluoride concentration (20 mg/L). In addition, exposure to 20 mg/L fluoride induced significantly higher MDA levels compared with that in the control group. Remarkably, compared with the 20 mg/L NaF group, SOD activity and T-AOC increased sharply, and the levels of NO and MDA decreased sharply with selenium intervention. Therefore, we speculated that selenium effectively relieves fluoride-induced toxicity and oxidative stress in NRK-52E cells.

Effect of NaF and/or Na₂SeO₃ on ΔΨ_m in NRK-52E Cells

The ΔΨ_m of NRK-52E cells was analyzed by JC-1, a fluorescent dye. JC-1 is capable of selectively entering mitochondria, where it forms aggregates and gives off red fluorescence when the ΔΨ_m is relatively high. By contrast, the monomeric form shows green fluorescence. We found that the percentage of cells with green fluorescence increased with NaF concentration (Fig. 4a (A1,

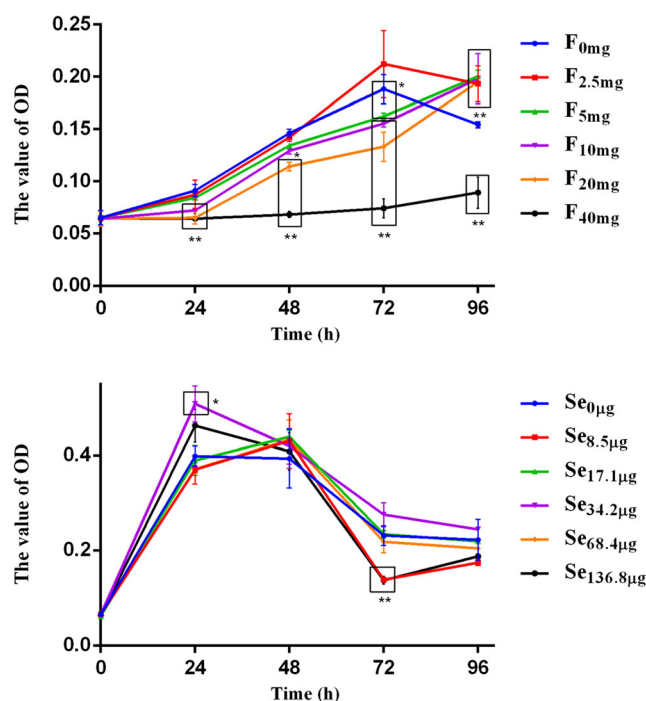
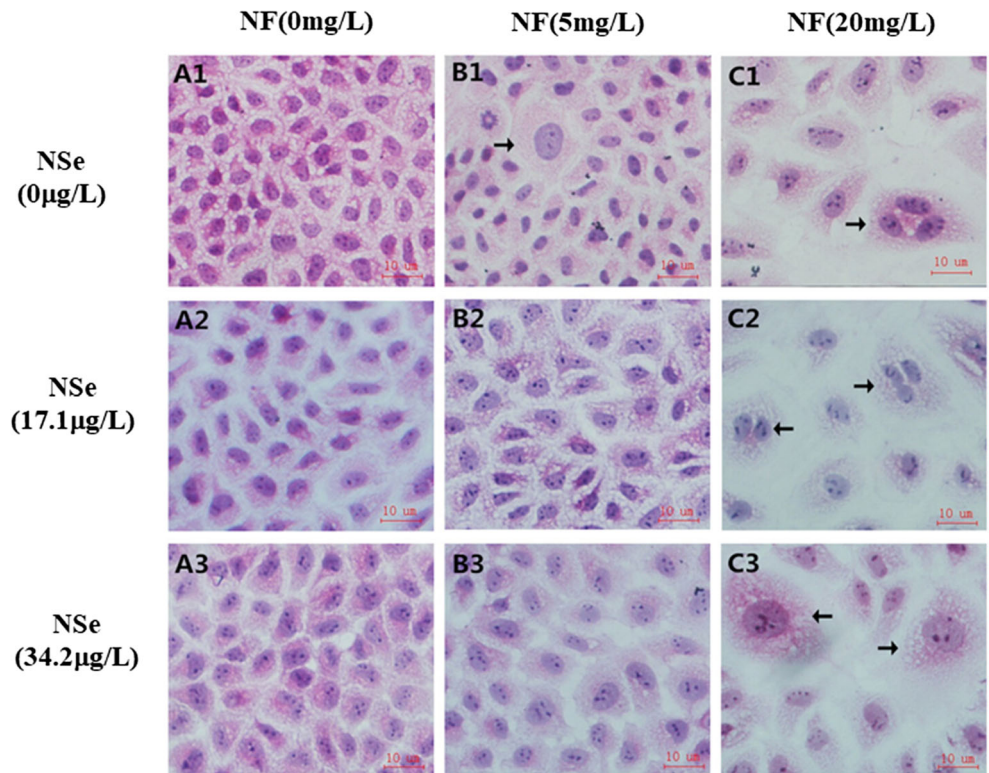


Fig. 1 Proliferation of NRK-52E cells exposed to NaF and Na₂SeO₃. **P* < 0.05 and ***P* < 0.01 vs. Control

Fig. 2 Histopathological changes in NRK-52E cells exposed to NaF and Na₂SeO₃. Magnification, × 400. LF (low fluoride dosage of 5 mg/L), HF (high fluoride dosage of 20 mg/L), LS (low selenium dosage of 17.1 μg/L), HS (high selenium dosage of 34.2 μg/L)



B1, and C1)). Remarkably, compared with NaF (5 and 20 mg/L), the percentage of cells with green

fluorescence was decreased when the cells were treated with Na₂SeO₃ at 17.1 and 34.2 μg/L (Fig. 4b).

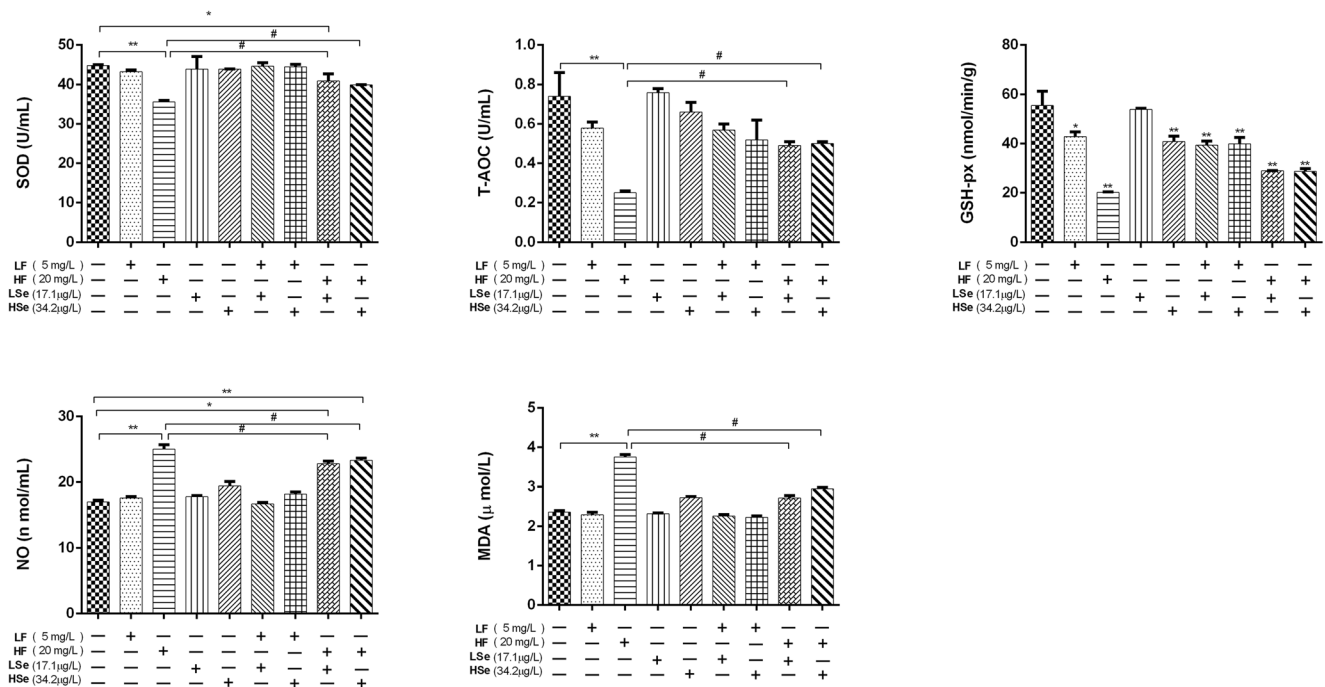


Fig. 3 Effect of selenium on SOD, GSH-px, T-AOC, NO, and MDA in fluoride-treated NRK-52E cells. The values represent the mean ± standard deviation (n = 6). *P < 0.05 and **P < 0.01 vs. control; #P < 0.05 vs.

the corresponding selenium intervention group. LF (low fluoride dosage of 5 mg/L), HF (high fluoride dosage of 20 mg/L), LS (low selenium dosage of 17.1 μg/L), HS (high selenium dosage of 34.2 μg/L)

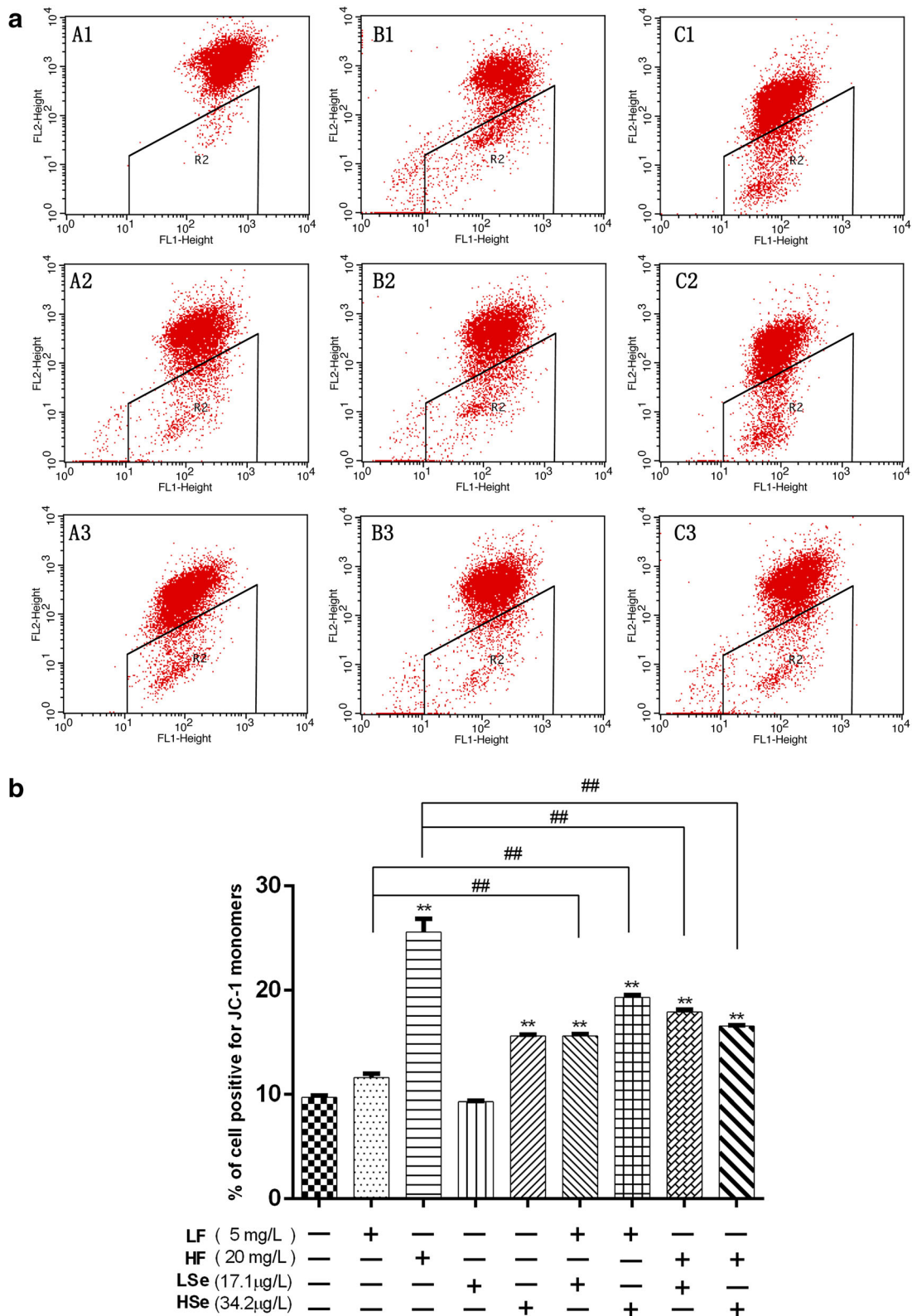


Fig. 4 Flow cytometry detection of mitochondrial membrane potential by the JC-1 assay. Cells in the R2 area represents the ratio of JC-1 conversion from polymeric to monomeric form. The values represent the mean \pm standard deviation ($n = 6$). * $P < 0.05$ and ** $P < 0.01$ vs. control;

$P < 0.05$ and ## $P < 0.01$ vs. the corresponding selenium intervention group. LF (low fluoride dosage of 5 mg/L), HF (high fluoride dosage of 20 mg/L), LS (low selenium dosage of 17.1 μg/L), HS (high selenium dosage of 34.2 μg/L)

Effect of NaF and/or Na₂SeO₃ on NRK-52E Cell Apoptosis

Figure 5 shows the effect of selenium intervention on chronic fluoride-induced apoptosis of NRK-52E cells. Almost all cells in the control group (Fig. 5a (A1)) were located in the lower left area, whereas cells in the fluoride group (Fig. 5a (B1 and C1)) were located in the upper right area, indicating that most fluoride-treated cells were nonviable, apoptotic, or dying. Compared with the control group, the proportion of apoptotic cells was significantly elevated after fluoride treatment, but with selenium intervention, the number of apoptotic cells was observably reduced (Fig. 5b).

Effect of NaF and/or Na₂SeO₃ on mRNA Expression of Bad, Bcl-2, Bax, Caspase-3, Caspase-8, and Caspase-9

To gain further insight into the mechanisms of apoptosis underlying the effect of NaF and Na₂SeO₃ on NRK-52E cells, we assessed the mRNA expression of genes encoding Bad, Bcl-2, Bax, caspase-3, caspase-8, and caspase-9 (Fig. 6). An obvious increase in the expression of these apoptosis-related genes was observed with increasing NaF concentration (0, 5, and 20 mg/L). Compared with the 20 mg/L NaF group, the mRNA levels of Bad, Bax, caspase-3, caspase-8, and caspase-9 were highly decreased with Na₂SeO₃ intervention.

Effect of NaF and/or Na₂SeO₃ on Protein Levels of Bax and Bcl-2

We evaluated the protein levels of Bax and Bcl-2 to examine the effect of NaF and Na₂SeO₃ on NRK-52E cell apoptosis. Compared with the control group, the expression of Bcl-2 was obviously decreased in the high fluoride treatment group, whereas Bax expression was visibly elevated in the fluoride groups. Compared with the 20 mg/L NaF group, the protein level of Bcl-2 was highly elevated, whereas that of Bax was visibly decreased with Na₂SeO₃ intervention (Fig. 7).

Discussion

An increasing number of experimental studies have revealed that chronically NaF-intoxicated rats experienced changes in renal function and histology, interstitial edema, tubular destruction, inflammation, fibrosis, glomerular, and medullary hyperemia [17, 18]. Notably, selenium is beneficial to human and animal health, and some reports have indicated that selenium alleviated fluoride-induced toxicity in rats [11–13]. However, knowledge on the mechanisms underlying the protective effect of selenium against sodium fluoride nephrotoxicity is relatively limited.

Excessive fluoride intake over a long period of time may result in fluorosis, a severe public health problem that occurs when the daily fluoride intake exceeds 20 mg [19]. Selenium is a necessary cofactor for numerous selenoenzymes. However, the range between nutritional and toxic doses of selenium is narrow [15]. When using selenium as a nutritional supplement, its safety limits and potential toxic effects are first considered. We thus examined the proliferation of NRK-52E cells by MTT assay after they were treated with NaF or Na₂SeO₃ at different concentrations and identified the optimal concentrations of NaF and Na₂SeO₃. From the results, the NaF concentrations used in this study were chosen to be 5 and 20 mg/L, and 17.1 and 34.2 µg/L were selected as the effective doses of selenium. In addition, an exposure time of 48 h was used in further studies. The kidney is the primary organ involved in the excretion and retention of fluoride. Studies have found that this sensitive organ exhibits histopathological and functional responses to excessive amounts of fluoride [18, 20, 21]. In this study, we observed that the morphology of renal tubular epithelial cells was significantly altered with increasing NaF concentration, showing enlarged cell volume and nuclei, wide intercellular space, and decreased cell adhesion. Interestingly, cell damage caused by fluoride was effectively alleviated after selenium intervention.

Previous studies have demonstrated the relationship between fluoride toxicity and oxidative stress in renal tissues [21], and the generation of free radicals is an important mechanism in fluoride-induced toxicity [22]. In addition, changes in the antioxidant defense system and lipid peroxidation play important roles in the toxic effects of fluoride [23–26]. Nitric oxide synthase (NOS) is one of the main sources of reactive oxygen species [21, 27]. Studies have found that most cytotoxic effects of fluoride are mediated by the production of NO. Reactive oxygen species are important and cause NOS phosphorylation [28]. As the end product of lipid peroxidation, MDA is commonly used as an indicator of oxidative stress [29]. Antioxidant enzymes are an important element of antioxidant defense, wherein SOD, GSH-px, and T-AOC play a principal role in preventing free radical accumulation [30]. Increased SOD and GSH-px activity and T-AOC exert protection against oxidant impairment. In the present study, selenium administration after NaF treatment attenuated oxidative stress, which was manifested as a decrease in the levels of MDA and NO and an increase in SOD and GSH-px activity and T-AOC. These findings indicated that the protective effects of selenium on NRK-52E cells were partially attributed to the free radical-scavenging activity and enhanced antioxidant defense system. The data clearly demonstrated that selenium significantly improved the antioxidant defense mechanisms against renal fluorosis *in vitro*.

Apoptosis plays a key role in normal body development. However, abnormal apoptosis is a basic feature of a wide variety of acute and chronic diseases. Mounting evidence

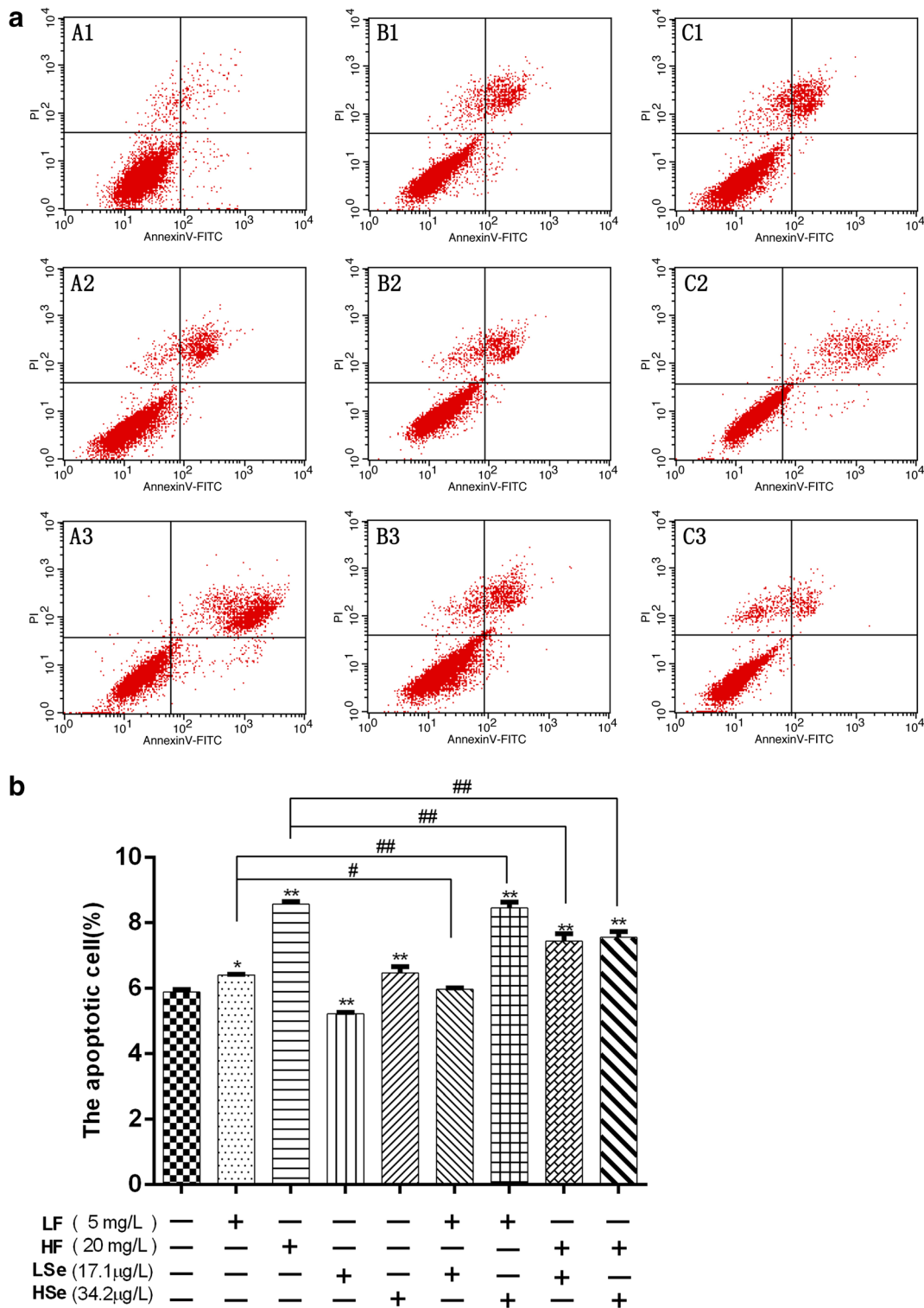


Fig. 5 Flow cytometry detection of apoptosis by Annexin V-FITC and PI double staining. Annexin V-positive (early apoptotic) cells, PI-positive (necrotic) cells, and Annexin V and PI double-positive (late apoptotic) cells are shown in flow cytometric analysis. * $P < 0.05$ and ** $P < 0.01$ vs.

control; # $P < 0.05$ and ## $P < 0.01$ vs. the corresponding selenium intervention group. LF (low fluoride dosage of 5 mg/L), HF (high fluoride dosage of 20 mg/L), LS (low selenium dosage of 17.1 μg/L), HS (high selenium dosage of 34.2 μg/L)

has shown that oxidative stress mediates apoptosis through various channels, such as proteins in the Bcl-2 and caspase

family [31]. The $\Delta\psi_m$ may be regulated by the Bcl-2 family of proteins, and the loss of $\Delta\psi_m$ is a consequence of

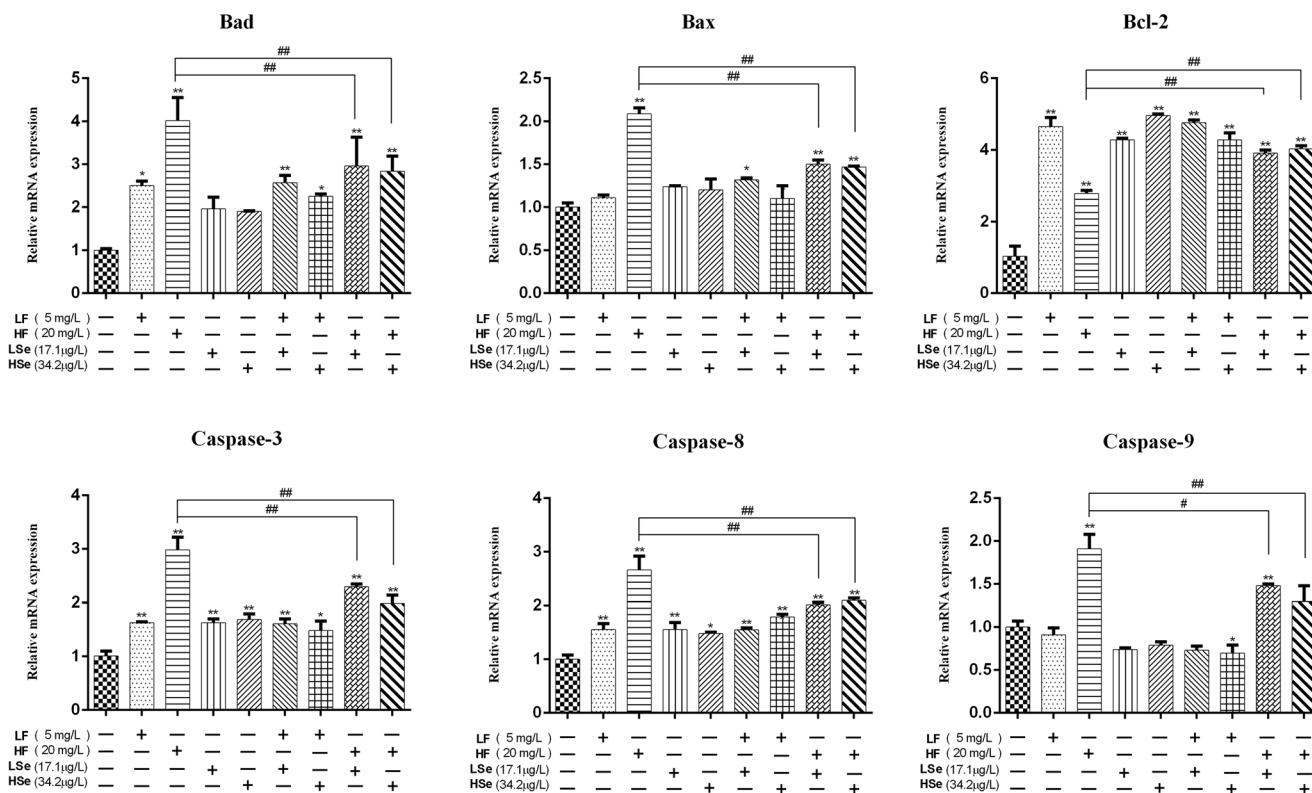


Fig. 6 Fold change in the mRNA expression of Bcl-2, Bax, Bad, caspase-8, caspase-9, and caspase-3 assessed using the $2^{-\Delta\Delta Ct}$ method. The values represent the mean \pm standard deviation ($n = 6$). * $P < 0.05$ and ** $P < 0.01$ vs. control; # $P < 0.05$ and ## $P < 0.01$ vs. the corresponding selenium intervention

group. LF (low fluoride dosage of 5 mg/L), HF (high fluoride dosage of 20 mg/L), LS (low selenium dosage of 17.1 μg/L), HS (high selenium dosage of 34.2 μg/L)

apoptotic signaling [32–34]. Oxidative stress is closely related to damages in cellular DNA and mitochondrial membrane,

which may cause apoptosis [35, 36]. It also results in excessive reactive oxygen species formation, which leads to cellular

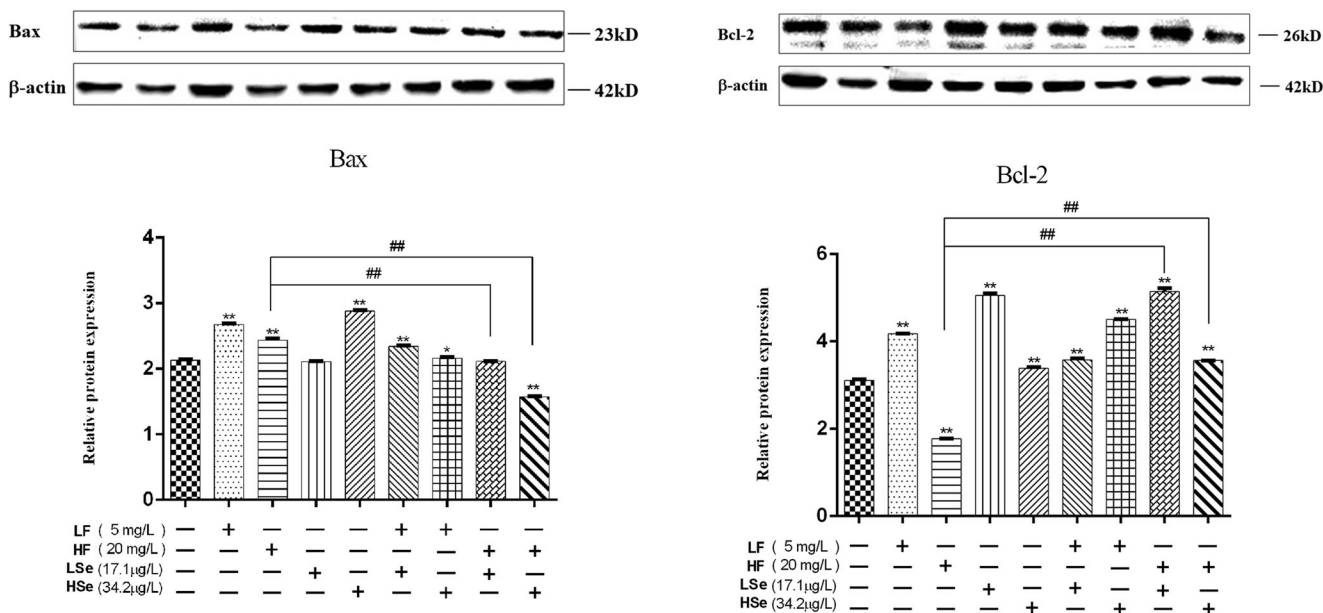


Fig. 7 The protein expression levels of Bcl-2 and Bax were analyzed using Western blotting. The values represent the mean \pm standard deviation ($n = 6$). * $P < 0.05$ and ** $P < 0.01$ vs. control; # $P < 0.05$ and ## $P < 0.01$ vs. the corresponding selenium intervention group. LF (low

fluoride dosage of 5 mg/L), HF (high fluoride dosage of 20 mg/L), LS (low selenium dosage of 17.1 μg/L), HS (high selenium dosage of 34.2 μg/L)

injury and apoptosis [37]. Our flow cytometry results revealed that the degree of NRK-52E cell apoptosis was significantly elevated after 48 h of NaF treatment. However, selenium at different doses inhibited fluorosis-induced NRK-52E cell apoptosis. Apoptosis is closely related to $\Delta\Psi_m$ stability, and when the $\Delta\Psi_m$ collapses, apoptosis is irreversible [36, 38]. Our studies confirmed that fluoride treatment induced the depolarization of $\Delta\Psi_m$, but this was prevented by selenium administration.

Apoptosis is mainly regulated by proteins in the Bcl-2 and caspase family [39–41]. Bcl-2 is an anti-apoptotic protein that regulates cell apoptosis either by preventing the release of cytochrome c from the mitochondria into the cytosol or by binding to apoptosis-activating factors [42]. The balance between the anti-apoptotic member Bcl-2 and the pro-apoptotic member Bax is essential for normal apoptotic signaling [43, 44]. We observed that fluoride disrupted the balance between Bcl-2 and Bax, and the change in $\Delta\Psi_m$ was consistent with the results of apoptosis. Our data also indicated that at certain concentrations, selenium reduced Bax expression, increased Bcl-2 expression, and prevented $\Delta\Psi_m$ depolarization. The pro-apoptotic caspase family plays a vital role in the process of apoptosis and includes the intracellular initiator caspase-9 and the extracellular initiator caspase-8 and effector caspase-3 [14, 19]. Caspase-9 is a mediator of the intrinsic pathway, which can be activated by hypoxia and oxidative stress. Caspase-8 is the key promoter in the death receptor-mediated apoptotic pathway. Caspase-3 is a member of the cysteine proteases family and is responsible for the cleavage of key cellular proteins, which leads to typical morphological changes in cells undergoing apoptosis [44]. Upregulation of caspase-9 and caspase-8 promotes caspase-3 expression, eventually leading to cell apoptosis. In this study, NRK-52E cells treated with NaF showed increased expression of caspase-8, caspase-9, and caspase-3. Conversely, the activity of caspase-9, caspase-8, and caspase-3 was decreased after NaF-induced cells were treated with Na_2SeO_3 , confirming the potential protective property of selenium. This property was confirmed by the results of NRK-52E cell apoptosis. Our findings suggest that the Bcl-2 protein family and caspase pathway play a critical role in the protective effect of selenium in renal cells.

In conclusion, selenium exerted remarkable protective effects against NaF-induced apoptosis and oxidative stress and changes in the expression of mRNA and proteins in the Bcl-2/caspase family, indicating that selenium might be effective in renal fluorosis treatment in vitro. The precise mechanism underlying the inhibitory effects of selenium on fluoride-induced apoptosis will be investigated in future studies.

Funding Information This work was financed by grants from the China National Natural Science Foundation (No.31240009), the Special Funds for Experimental Animal Technologies in Shanxi Province of China (No.2012K02), and the Shanxi Scholarship Council of China (Grant No.2016-056).

Compliance with Ethical Standards

Conflict of Interest The authors declare that they have no conflict of interest.

References

- Chen L, Chen HQ, Yao C, Chang C, Xia HC, Zhang CX, Zhou Y, Yao Q, Chen KP (2015) The toxicity of NaF on BmN cells and a comparative proteomics approach to identify protein expression changes in cells under NaF-stress: impact of NaF on BmN cells. *J Hazard Mater* 286(9):624–631. <https://doi.org/10.1016/j.jhazmat.2014.12.056>
- WHO (1993) Guidelines for Drinking Water Quality, 45. World Health Organization, Geneva
- Luo Q, Guo HR, Kuang P, Cui HM, Deng HD, Liu H, Lu YJ, Wei Q, Chen LL, Fang J, Zuo ZC, Deng JJ, Li YL, Wang X, Zhao L (2018) Sodium fluoride arrests renal G2/M phase cell-cycle progression by activating ATMChk2-P53/Cdc25C signaling pathway in mice. *Cell Physiol Biochem* 51(5):2421–2433. <https://doi.org/10.1159/000495899>
- Tang WHW, Li DY, Hazen SL (2019) Dietary metabolism, the gut microbiome, and heart failure. *Nat Rev Cardiol* 16(3):137–154. <https://doi.org/10.1038/s41569-018-0108-7>
- Usuda K, Kono K, Dote T, Nishiura K, Miyata K, Nishiura H, Shimahara M, Sugimoto K (1998) Urinary biomarkers monitoring for experimental fluoride nephrotoxicity. *Arch Toxicol* 72(2):104–109. <https://doi.org/10.1007/s002040050475>
- Cao J, Chen J, Wang J, Jia R, Xue W, Luo Y, Gan X (2013) Effects of fluoride on liver apoptosis and Bcl-2, Bax protein expression in freshwater teleost, *Cyprinus carpio*. *Chemosphere* 91(8):1203–1212. <https://doi.org/10.1016/j.chemosphere.2013.01.037>
- Zhang Z, Zhou B, Wang H, Wang F, Song Y, Liu S, Xi S (2014) Maize purple plant pigment protects against fluoride-induced oxidative damage of liver and kidney in rats. *Int J Environ Res Public Health* 11(1):1020–1033. <https://doi.org/10.3390/ijerph110101020>
- Dong N, Feng J, Xie J, Tian X, Li M, Liu P, Zhao Y, Wei C, Gao Y, Li B, Qiu Y, Yan X (2019) Co-exposure to arsenic-fluoride results in endoplasmic reticulum stress-induced apoptosis through the PERK signaling pathway in the liver of offspring rats. <https://doi.org/10.1007/s12011-019-01975-1>
- Alhusaini AM, Faddah LM, El Orabi NF, Hasan IH (2018) Role of some natural antioxidants in the modulation of some proteins expressions against sodium fluoride-induced renal injury. *Biomed Res Int* 2018:5614803. [10.1155/2018/5614803](https://doi.org/10.1155/2018/5614803), 9
- Naziroglu M (2009) Role of selenium on calcium signaling and oxidative stress-induced molecular pathways in epilepsy. *Neurochem Res* 34(12):2181–2191. <https://doi.org/10.1007/s11064-009-0015-8>
- Zheng X, Sun Y, Ke L, Ouyang W, Zhang Z (2016) Molecular mechanism of brain impairment caused by drinking-acquired fluorosis and selenium intervention. *Environ Toxicol Pharmacol* 43: 134–139. <https://doi.org/10.1016/j.etap.2016.02.017>
- Miao K, Zhang L, Yang S, Qian W, Zhang Z (2013) Intervention of selenium on apoptosis and Fas/FasL expressions in the liver of fluoride-exposed rats. *Environ Toxicol Pharmacol* 36(3):913–920. <https://doi.org/10.1016/j.etap.2013.08.003>
- Qian W, Miao K, Li T, Zhang Z (2013) Effect of selenium on fluoride-induced changes in synaptic plasticity in rat hippocampus. *Biol Trace Elem Res* 155(2):253–260. <https://doi.org/10.1007/s12011-013-9773-x>
- Feng P, Wei JR, Zhang ZG (2012) Influence of selenium and fluoride on blood antioxidant capacity of rats. *Experimental and*

- toxicologic pathology: official journal of the Gesellschaft für Toxikologische Pathologie 64(6):565–568. <https://doi.org/10.1016/j.etp.2010.11.014>
15. Wang GZ, Niu ZX (2011) The progress study of toxicity of selenium. *Northwest Pharm J* 25(3):237–238
 16. Rayman MP (2000) The importance of selenium to human health. *Lancet* (London, England) 356(9225):233–241. [https://doi.org/10.1016/S0140-6736\(00\)02490-9](https://doi.org/10.1016/S0140-6736(00)02490-9)
 17. Dharmaratne RW (2019) Exploring the role of excess fluoride in chronic kidney disease: a review. *Hum Exp Toxicol* 38(3):269–279. <https://doi.org/10.1177/0960327118814161>
 18. Tian X, Feng J, Dong N, Lyu Y, Wei C, Li B, Ma Y, Xie J, Qiu Y, Song G, Ren X, Yan X (2019) Subchronic exposure to arsenite and fluoride from gestation to puberty induces oxidative stress and disrupts ultrastructure in the kidneys of rat offspring. *Sci Total Environ* 686:1229–1237. <https://doi.org/10.1016/j.scitotenv.2019.04.409>
 19. Dhar V, Bhatnagar M (2009) Physiology and toxicity of fluoride. *Indian J Dent Res* 20:350–355
 20. Xu H, Hu LS, Chang M, Jing L, Zhang XY, Li GS (2005) Proteomic analysis of kidney in fluoride-treated rat. *Toxicol Lett* 160(1):69–75. <https://doi.org/10.1016/j.toxlet.2005.06.009>
 21. Nabavi SF, Moghaddam AH, Eslami S, Nabavi SM (2012) Protective effects of curcumin against sodium fluoride-induced toxicity in rat kidneys. *Biol Trace Elem Res* 145(3):369–374. <https://doi.org/10.1007/s12011-011-9194-7>
 22. Ke L, Zheng X, Sun Y, Ouyang W, Zhang Z (2016) Effects of sodium fluoride on lipid peroxidation and PARP, XBP-1 expression in PC12 cell. *Biol Trace Elem Res* 173(1):161–167. <https://doi.org/10.1007/s12011-016-0641-3>
 23. Akdogan M, Kaleli S, Yazar H, Desdicioglu R, Yuvaci H (2016) Effect of high-dose fluoride on antioxidant enzyme activities of amniotic fluid in rats. *JPMA J Pakistan Medical Assoc* 66(4):435–438
 24. Nabavi SM, Habtemariam S, Nabavi SF, Sureda A, Daglia M, Moghaddam AH, Amani MA (2013) Protective effect of gallic acid isolated from *Peltiphyllyllum peltatum* against sodium fluoride-induced oxidative stress in rat's kidney. *Mol Cell Biochem* 372(1–2):233–239. <https://doi.org/10.1007/s11010-012-1464-y>
 25. Baba N, Raina R, Verma P, Sultana M (2016) Free radical-induced nephrotoxicity following repeated oral exposure to chlorpyrifos alone and in conjunction with fluoride in rats. *Turkish J Med Sci* 46(2):512–517. <https://doi.org/10.3906/sag-1403-109>
 26. Shuhua X, Ziyou L, Ling Y, Fei W, Sun G (2012) A role of fluoride on free radical generation and oxidative stress in BV-2 microglia cells. *Mediat Inflamm* 2012:102954. [10.1155/2012/102954](https://doi.org/10.1155/2012/102954), 8
 27. Zhang H, Zhang HM, Wu LP, Tan DX, Kamat A, Li YQ, Katz MS, Abboud HE, Reiter RJ, Zhang BX (2011) Impaired mitochondrial complex III and melatonin responsive reactive oxygen species generation in kidney mitochondria of db/db mice. *J Pineal Res* 51(3):338–344. <https://doi.org/10.1111/j.1600-079X.2011.00894.x>
 28. Bergandi L, Aina V, Malavasi G, Morterra C, Ghigo D (2011) The toxic effect of fluoride on MG-63 osteoblast cells is also dependent on the production of nitric oxide. *Chem Biol Interact* 190(2–3):179–186. <https://doi.org/10.1016/j.cbi.2011.02.003>
 29. Macotpet A, Suksawat F, Sukon P, Pimpakdee K, Pattarapanwichien E, Tangrassameeprasert R, Boonsiri P (2013) Oxidative stress in cancer-bearing dogs assessed by measuring serum malondialdehyde. *BMC Vet Res* 9:101. <https://doi.org/10.1186/1746-6148-9-101>
 30. Hassan HA, Abdel-Aziz AF (2010) Evaluation of free radical-scavenging and anti-oxidant properties of black berry against fluoride toxicity in rats. *Food and chemical toxicology: an international journal published for the British Industrial Biological Research Association* 48(8–9):1999–2004. <https://doi.org/10.1016/j.fct.2010.05.018>
 31. Cheng EH, Kirsch DG, Clem RJ, Ravi R, Kastan MB, Bedi A, Ueno K, Hardwick JM (1997) Conversion of Bcl-2 to a Bax-like death effector by caspases. *Science* (New York, NY) 278(5345):1966–1968. <https://doi.org/10.1126/science.278.5345.1966>
 32. Lopez J, Tait SW (2015) Mitochondrial apoptosis: killing cancer using the enemy within. *Br J Cancer* 112(6):957–962. <https://doi.org/10.1038/bjc.2015.85>
 33. Sharpe JC, Amoult D, Youle RJ (2004) Control of mitochondrial permeability by Bcl-2 family members. *Biochim Biophys Acta* 1644(2–3):107–113. <https://doi.org/10.1016/j.bbamer.2003.10.016>
 34. Hu XY, Liang JY, Guo XJ, Liu L, Guo YB (2015) 5-Fluorouracil combined with apigenin enhances anticancer activity through mitochondrial membrane potential (DeltaPsi_m)-mediated apoptosis in hepatocellular carcinoma. *Clin Exp Pharmacol Physiol* 42(2):146–153. <https://doi.org/10.1111/1440-1681.12333>
 35. Zhang L, Cheng X, Gao Y, Bao J, Guan H, Lu R, Yu H, Xu Q, Sun Y (2016) Induction of ROS-independent DNA damage by curcumin leads to G2/M cell cycle arrest and apoptosis in human papillary thyroid carcinoma BCPAP cells. *Food Funct* 7(1):315–325. <https://doi.org/10.1039/c5fo00681c>
 36. Park C, Cha HJ (2019) Protective effect of phloroglucinol on oxidative stress-induced DNA damage and apoptosis through activation of the Nrf2/HO-1 signaling pathway in HaCaT human keratinocytes. *Mar Drugs* 17(4):225. <https://doi.org/10.3390/md17040225>
 37. Wang YX, Xiao X, Zhan XA (2018) Antagonistic effects of different selenium sources on growth inhibition, oxidative damage, and apoptosis induced by fluorine in broilers. *Poult Sci* 97(9):3207–3217. <https://doi.org/10.3382/ps/pey19>
 38. Yan X, Wang L, Yang X, Qiu Y, Tian X, Lv Y, Tian F, Song G, Wang T (2017) Fluoride induces apoptosis in H9c2 cardiomyocytes via the mitochondrial pathway. *Chemosphere* 182:159–165. <https://doi.org/10.1016/j.chemosphere.2017.05.002>
 39. Eno CO, Zhao G, Olberding KE, Li C (2012) The Bcl-2 proteins Noxa and Bcl-xL co-ordinately regulate oxidative stress-induced apoptosis. *Biochem J* 444(1):69–78. <https://doi.org/10.1042/bj20112023>
 40. Fan D, Fan TJ (2017) Clonidine induces apoptosis of human corneal epithelial cells through death receptors-mediated, mitochondria-dependent signaling pathway. *Toxicol Sci* 156(1):252–260. <https://doi.org/10.1093/toxsci/kfw249>
 41. Ying J, Xu J, Shen LP, Mao ZJ, Liang JC, Lin SX, Yu XY, Pan RW, Yan CX, Li SB, Bao QY, Li PZ (2017) The effect of sodium fluoride on cell apoptosis and the mechanism of human lung BEAS-2B cells in vitro. *Biol Trace Elem Res* 179:59–69. <https://doi.org/10.1007/s12011-017-0937-y>
 42. Desagher S, Martinou JC (2000) Mitochondria as the central control point of apoptosis. *Trends Cell Biol* 10(9):369–377. [https://doi.org/10.1016/S0962-8924\(00\)01803-1](https://doi.org/10.1016/S0962-8924(00)01803-1)
 43. Siddiqui WA, Ahad A, Ahsan H (2015) The mystery of BCL2 family: Bcl-2 proteins and apoptosis: an update. *Arch Toxicol* 89(3):289–317. <https://doi.org/10.1007/s00204-014-1448-7>
 44. Li WS, Jiang BH, Cao XL, Xie YJ, Huang T (2017) Protective effect of lycopene on fluoride-induced ameloblasts apoptosis and dental fluorosis through oxidative stress-mediated Caspase pathways. *Chemico-biological interactions* 261:27–34. <https://doi.org/10.1016/j.cbi.2016.11.021>

Publisher's Note Springer Nature remains neutral with regard to jurisdictional claims in published maps and institutional affiliations.